Progress In Electromagnetics Research C, Vol. 17, 39–53, 2010

EXPERIMENTAL VERIFICATION OF ULTRA-WIDE-BAND PULSE RADIATION FROM MONOPOLE ARRAY ANTENNAS

K. Rambabu, A. E.-C. Tan, and K. K.-M. Chan

Electrical and Computer Engineering
University of Alberta, Edmonton, Alberta T6G2V4, Canada

M. Y.-W. Chia

Institute for Infocomm Research
Agency for Science, Technology and Research, 138632, Singapore

Abstract—In this paper, a time domain analysis for ultra-wideband short pulse radiation from wire monopole antennas and their arrays is presented. The pulse travels along the monopole antenna and reflects from the open end; during the pulse reflection, the pulse gets compressed. The analysis presented in this paper accounts for the pulse compression and the radiated pulse is compared with the measured pulse. Measured energy patterns for different pulse excitations of the monopole and monopole arrays are presented and compared with theoretical patterns.

1. INTRODUCTION

Ultra-wideband (UWB) antenna design and analysis require an extension to conventional antenna theory, i.e., from steady state to transient conditions. Radiation of a UWB signal (short-pulse) is different from a narrowband signal. Narrowband radiation occurs on the entire length (aperture) of the antenna, whereas a UWB signal radiates from the centre and edges of the antenna aperture. The narrowband radiated signals will be in the form of the derivative of the exciting currents, whereas UWB signals have their radiated fields in the form of repeated exciting currents [1]. The amplitude of the UWB radiation depends not only on angular coordinates but also on

Received 12 July 2010, Accepted 26 October 2010, Scheduled 3 November 2010
Corresponding author: Adrian Eng Choon Tan (aetan@ualberta.ca).

time. Kanda has shown that the transmitting transient response of an antenna is proportional to the time derivative of the receiving transient response of the same antenna [2], i.e., there will be an extra $j\omega$ factor in the antenna reciprocity relationship. For narrowband radiation the $j\omega$ term becomes a 90 deg phase shift. So the sine term becomes a cosine term, in classical frequency domain it can be ignored. Therefore, the gain of a UWB antenna in the receiving and transmitting modes is different, integration and differentiation depending on mode of the antenna, due to $j\omega$ term.

The growing interest in the radiation and detection of short pulses with ultra wide bandwidths has made an impact on the time-domain analysis of UWB antennas. One way of analyzing the radiation and detection of these pulses would involve the traditional frequency domain antenna parameters on a frequency by frequency basis [3]. However, because of the broad frequency band of the short pulse, direct treatment of the antennas in the time domain may lead to more efficient and physically transparent representations.

The phase centre of the antenna is the apparent point from which the antenna radiates at a specified frequency. This radiating centre is often a function of frequency and is an important aspect of UWB antennas. Log-periodic dipole arrays and many horns have a phase center that varies with frequency [4]. On the other hand, some wire antennas such as dipoles and monopoles have a phase center that remains stationary with frequency. Monopoles are the building blocks of these wire antennas.

The transient behaviour of the radiated and received fields associated with resistively loaded dipoles has been studied in [5]. Frequency domain expressions for the current distribution and radiated fields that have been derived in [6] are used to obtain the corresponding time domain representations by evaluating the associated inverse Fourier transform. The transient radiation characteristics of an optimized ultra wideband printed dipole antenna is simulated and presented in [7]. In [8], an investigation, based on electromagnetic simulations, is conducted into the use of suboptimal planar dipoles to radiate ultra-wideband pulses. In this investigation, the excited pulse is shorter than the length of the antenna. In this paper, we present time domain analysis for short pulse radiation from monopole antennas and their arrays.

2. THEORY

Consider an infinitesimally thin wire antenna of length L (either dipole or monopole) as shown in Figure 1. Assume the spatial width ($c\tau$)

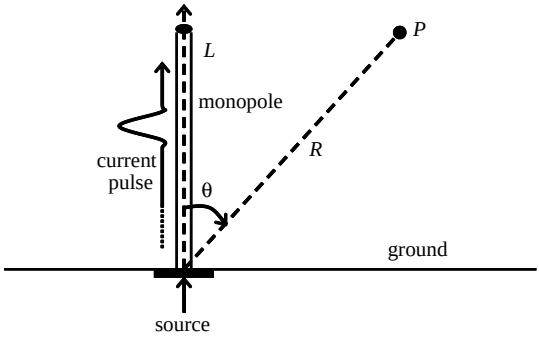

Figure 1. Monopole antenna.

and τ pulse duration of the exciting pulse is much smaller than the antenna length. This analysis assumes that the pulse shape is not distorted along the antenna. The excited current pulse will travel along the antenna, get reflected at the end of the antenna, and then travel back into the source, therefore radiation occurs at multiple times. The radiation due to the antenna is the vectorial sum of the radiations from small current elements along the length of the antenna.

The magnetic field (B) due to the infinitesimal conductor carrying current $i(t)$ is given by (Biot-Savarts law) [9]:

$$dB = \mu_0 i(t) \sin\theta / 4\pi R, \tag{1}$$

where θ is the angle with the axis of the monopole.

The corresponding electric field (time delayed) due to an infinitesimal current element (using Faraday's law) along the antenna, carrying current $i(t)$ is

$$dE = \frac{\mu_0}{4\pi R} \sin\theta \left\{ \partial i \left[t - \frac{l}{c} - \frac{R - l\cos\theta}{c} \right] / \partial t \right\}, \tag{2}$$

where c is the velocity of propagation. The velocity of propagation in wire and space is assumed uniform.

The radiated electric field is the time derivative of the excited current, but the total radiated field depends on the shape of the antenna and its dimensions. The total radiated electric field due to the monopole antenna of length L is

$$E = \int_0^L dE. \tag{3}$$

Using (2) the electric field can be written as

$$E = \frac{\mu_0}{4\pi R} \sin\theta \int_0^L \left\{ \frac{d}{dt} i \left[t - \frac{l}{c} - \frac{R - l\cos\theta}{c} \right] \right\} dl. \tag{4}$$

Using the Leibniz integral rule

$$E = \frac{\mu_0}{4\pi R} \sin\theta \frac{d}{dt} \left\{ \int_0^L i \left[t - \frac{l}{c} - \frac{R - l\cos\theta}{c} \right] dl \right\}. \tag{5}$$

The far field radiation (electric field) due to a wire antenna for an impulse excitation is

$$E = \frac{\eta}{4\pi R} \frac{\sin\theta}{\cos\theta - 1} \left\{ i\left(t - \frac{L}{c} - \frac{R - L\cos\theta}{c} \right) - i\left(t - \frac{R}{c} \right) \right\}, \tag{6}$$

where $\eta = \mu_0 c$.

Equation (6) shows that radiation occurs from the beginning and end of the wire antenna. However, the radiation occurs on entire length of the wire, the radiated fields of the inner sections of the wire have been canceled by the radiated fields of the adjacent sections. A similar expression has been derived in [10] with relativistic perspective.

It is very difficult to generate short pulses without distortion. Generally short pulses are associated with ringing; however Gaussian pulses and their derivatives can be generated with simple RF circuits with minimal ringing [11].

2.1. Gaussian Pulse Excitation

Let the exciting current pulse $i(t)$ be a Gaussian pulse with pulse width τ:

$$i(t) = e^{-(t/\tau)^2}. \tag{7}$$

The radiated electric field can be derived using (6) and (7)

$$\begin{aligned} E \;=\; & \frac{\eta}{4\pi R} \frac{\sin\theta}{\cos\theta - 1} \left\{ \exp\left[-\frac{1}{\tau^2} \left(t - \frac{L}{c} - \frac{R - L\cos\theta}{c} \right)^2 \right] \right. \\ & \left. - \exp\left[-\frac{1}{\tau^2} \left(t - \frac{R}{c} \right)^2 \right] \right\}. \end{aligned} \tag{8}$$

The radiated field depends on the length of the antenna. The effect of antenna length on the radiated electric field has been shown in Figure 2. The radiated electric field resembles the exciting currents for longer antenna lengths ($L > c\tau$) and it shows narrowband radiation characteristics: Radiated fields resemble the time derivative of exciting currents, at antenna length comparable to the spatial width of the pulse. Here the pulse width is assumed as 100 ps. Figure 3 shows the variation of the radiated fields in the elevation plane. Shape of the radiated pulse changes, getting compressed, as the elevation point approaches the axis of the antenna.

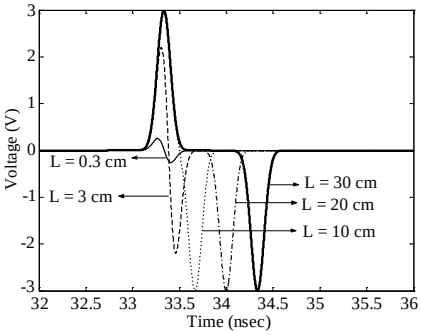

Figure 2. Effect of antenna length on the radiated fields for Gaussian excitation in the azimuth plane.

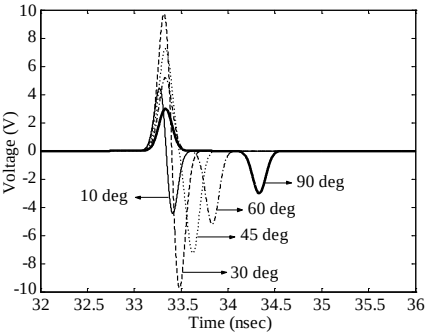

Figure 3. Radiated fields in the elevation plane for Gaussian excitation.

2.2. First Derivative Gaussian Pulse Excitation

This pulse is more suitable for radiation due to its zero DC value. The exciting current pulse $i(t)$ can be written as

$$i(t) = -(2t/\tau^2)e^{-(t/\tau)^2}. \tag{9}$$

The radiated electric field can be written as

$$\begin{aligned} E \;=\; & \frac{\eta}{4\pi R}\frac{\sin\theta}{\cos\theta - 1}\left\{-\frac{2[t - L/c - (R - L\cos\theta)/c]}{\tau^2}\right. \\ & \exp\left[-\left(\frac{t - L/c - (R - L\cos\theta)/c}{\tau}\right)^2\right] \\ & \left.+\frac{2(t - R/c)}{\tau^2}\exp\left[-\left(\frac{t - R/c}{\tau}\right)^2\right]\right\}. \end{aligned} \tag{10}$$

Figure 4 shows the effect of antenna length on the radiated fields and Figure 5 shows the variation of the electric field in the elevation plane.

2.3. Second Derivative Gaussian Pulse Excitation

This pulse has a symmetrical and narrow frequency spectrum compared with the other two Gaussian pulses. Its energy concentration is more towards higher frequencies of the spectrum. The second derivative Gaussian pulse can be represented by

$$i(t) = \frac{2}{\tau^2}\left(\frac{2t^2}{\tau^2} - 1\right)\exp\left(-\frac{t^2}{\tau^2}\right). \tag{11}$$

The radiated electric field will be

$$E = \frac{2\eta}{4\pi R\tau^2}\frac{\sin\theta}{\cos\theta - 1}\left\{\left(\frac{2[t - L/c - (R - L\cos\theta)/c]^2}{\tau^2} - 1\right)\right.$$
$$\exp\left(-\left(\frac{t - L/c - (R - L\cos\theta)/c}{\tau}\right)^2\right)$$
$$\left. - \left(\frac{2(t - R/c)^2}{\tau^2} - 1\right)\exp\left(-\left(\frac{t - R/c}{\tau}\right)^2\right)\right\}. \quad (12)$$

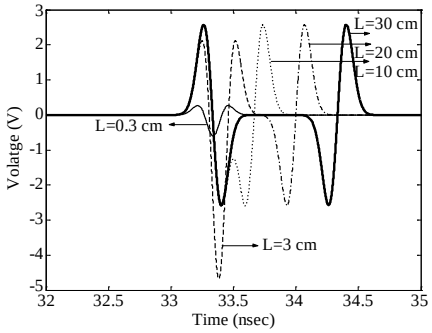

Figure 4. Effect of antenna length on radiated fields for first derivative Gaussian pulse excitation in the azimuth plane.

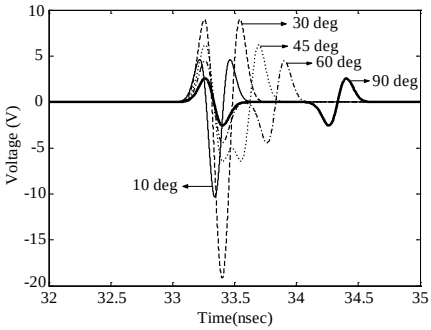

Figure 5. Radiated fields in the elevation plane for first derivative Gaussian pulse excitation.

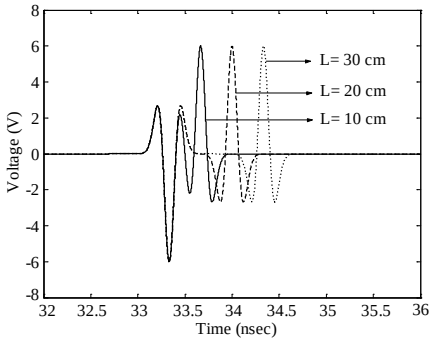

Figure 6. Effect of antenna length on the radiated fields for second derivative Gaussian pulse excitation in the azimuth plane.

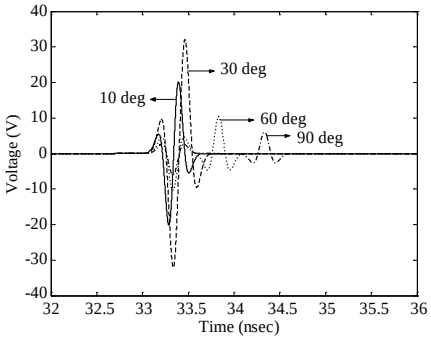

Figure 7. Radiated fields in the elevation plane for second derivative Gaussian pulse excitation.

Figures 6 and 7 show the radiated pulses with the antenna length and elevation angle variation respectively.

This analysis can be extended to an array of monopoles for short pulse excitation.

3. ARRAYS

3.1. Linear Arrays

Consider N monopoles separated by a distance d_v in a linear array. Let the length of each monopole be L and the excitation progressive delay is τ_l. The azimuth angle φ is measured with respect to the array axis, and θ is the elevation angle measured with respect to the monopole axis. This derivation assumes an identical current distribution on all elements, ignoring edge effects and coupling between antenna elements. The radiated electric field by the linear array is

$$E=\frac{\eta}{4\pi R}\frac{\sin\theta}{\cos\theta-1}\left\{\sum_{j=1}^{N}\left[i\left(t-\frac{L}{c}-\frac{R-L\cos\theta}{c}-\frac{(j-1)d_v\cos\varphi}{c}-(j-1)\tau_l\right)\right.\right.$$
$$\left.\left.-i\left(t-\frac{R}{c}-\frac{(j-1)d_v\cos\varphi}{c}-(j-1)\tau_l\right)\right]\right\}. \quad (13)$$

3.2. Planar Arrays

Consider a planar array antenna with M monopoles in a vertical column and N monopoles in horizontal row. The inter element

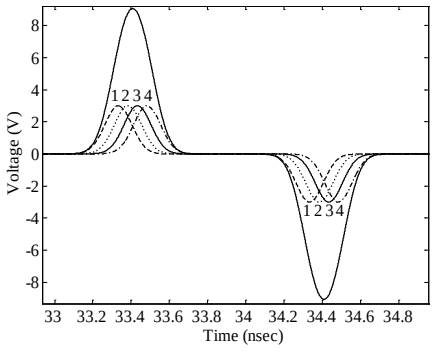

Figure 8. Radiated pulse in the azimuth plane of the linear array of monopoles.

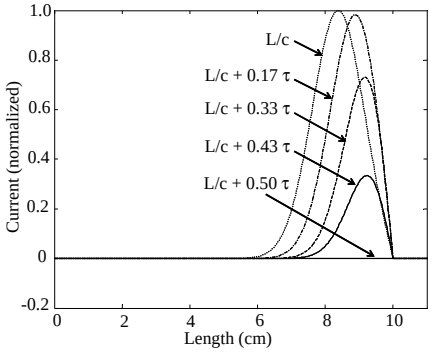

Figure 9. Pulse compression due to reflection at the end of an antenna.

spacing is d_v for vertical elements and d_h for horizontal elements. The progressive delay of the excitation is τ_v for vertical elements and τ_h for horizontal elements. The radiated electric field of the planar array can be written as

$$E = PQ, \tag{14}$$

$$\begin{aligned} P = {} & \frac{\eta}{4\pi R}\frac{\sin\theta}{\cos\theta - 1}\left[\sum_{j=1}^{M}\left(i\left(t - \frac{L}{c} - \frac{R - L\cos\theta}{c}\right.\right.\right. \\ & \left. - \frac{(j-1)d_v\cos\varphi\sin\theta}{c} - (j-1)\tau_v\right) \\ & \left.\left. - i\left(t - \frac{R}{c} - \frac{(j-1)d_v\cos\varphi\sin\theta}{c} - (j-1)\tau_v\right)\right)\right], \end{aligned} \tag{15}$$

$$\begin{aligned} Q = {} & \frac{\eta}{4\pi R}\frac{\sin\theta}{\cos\theta - 1}\left[\sum_{k=1}^{N}\left(i\left(t - \frac{L}{c} - \frac{R - L\cos\theta}{c}\right.\right.\right. \\ & \left. - \frac{(k-1)d_h\sin\varphi\sin\theta}{c} - (k-1)\tau_h\right) \\ & \left.\left. - i\left(t - \frac{R}{c} - \frac{(k-1)d_h\sin\varphi\sin\theta}{c} - (k-1)\tau_h\right)\right)\right], \end{aligned} \tag{16}$$

Figure 8 shows the radiated pulse, in the azimuth plane, of the linear array consisting of four monopoles with $L = 10\,\text{cm}$, $d = 2\,\text{cm}$, and $\tau_l = 0$. The total radiation of the array is the sum of the radiations of all monopoles in the array. The shape of the radiated pulse is influenced by all elements of the array. It is possible to shape the radiated pulse by choosing the inter element spacing and the progressive time delay of the excitation.

4. REFLECTING PULSE

When the incident pulse reaches the end of the wire antenna, the pulse gets reflected. To satisfy the boundary condition of the open end, the resultant current should be zero at the edge of the wire antenna. At the time of reflection, the pulse gets compressed to half of its width due to the open end of the antenna. Therefore, the radiation increases due to the sharp rise of the pulse. The compression of the pulse at the monopole edge ($L = 10\,\text{cm}$) has been shown in Figure 9.

The current pulse, which dwells on the last segment of the antenna at the time of reflection, can be written as

$$i'(t) = i(\tau - t) - i(t) \tag{17}$$

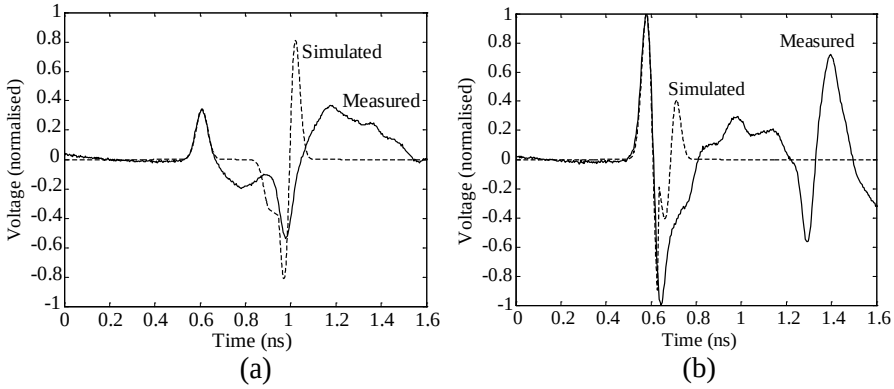

Figure 10. Simulated and measured radiated pulse in the (a) azimuth and (b) elevation planes for Gaussian pulse excitation.

for $L/c < t < L/c + \tau/2$. After reflection the pulse takes its original form and travels back to the source. While the pulse is getting reflected, the pulse dwells for a time $\tau/2$ on the last section of the antenna. The electric field radiated due to the compressed pulse (Gaussian pulse) is

$$E(t,\theta) = \frac{\mu_0}{4\pi R}\frac{d}{dt}\left[i'\left(t - \frac{L}{c} - \frac{R - L\cos\theta}{c}\right)\right]\sin\theta \tag{18}$$

for $(\frac{L}{c} + \frac{R-L\cos\theta}{c}) < t < (\frac{L}{c} + \frac{R-L\cos\theta}{c} + \frac{\tau}{2})$.

$$\begin{aligned} E \;=\; & \frac{\mu_0}{4\pi R}\sin\theta\left[\frac{2}{\tau^2}\left(t - \frac{L}{c} - \frac{R - L\cos\theta}{c}\right)\right. \\ & \exp\left[-\frac{1}{\tau^2}\left(t - \frac{L}{c} - \frac{R - L\cos\theta}{c}\right)^2\right] \\ & -\frac{2}{\tau^2}\left(\tau - t - \frac{L}{c} - \frac{R - L\cos\theta}{c}\right) \\ & \left.\exp\left[-\frac{1}{\tau^2}\left(\tau - t - \frac{L}{c} - \frac{R - L\cos\theta}{c}\right)^2\right]\right]. \end{aligned} \tag{19}$$

Figure 10(a) shows the measured and simulated radiated pulse of the monopole in the azimuth plane for Gaussian pulse excitation shown in Figure 11(a) ($\tau = 36$ ps). This radiation includes the radiation of the pulse due to reflection at the open end. The reflected signal travels back to the source; if the antenna and pulse source are not matched the pulse travels back and forth along the antenna resulting in multiple radiated pulses. The radiation between the peaks of the radiated pulse is due

to the ringing of the excitation pulse (c.f., Figure 11(a)). Figure 10(b) shows the simulated and measured radiated pulse of the monopole for a Gaussian pulse excitation in the elevation plane at $\theta = 30°$.

5. GENERATING DIFFERENT GAUSSIAN PULSES

Different Gaussian pulses have been generated by sending a step pulse through various differentiating circuits (high pass filters). To generate the approximate Gaussian pulse, a positive step of peak amplitude 10 V and rise time 45 psec has been sent through a high pass filter circuit. The output of the high pass filter is a Gaussian pulse of peak amplitude 1.4 V with $\tau = 36$ psec. By sending this Gaussian pulse through subsequent differentiators, first and second derivative

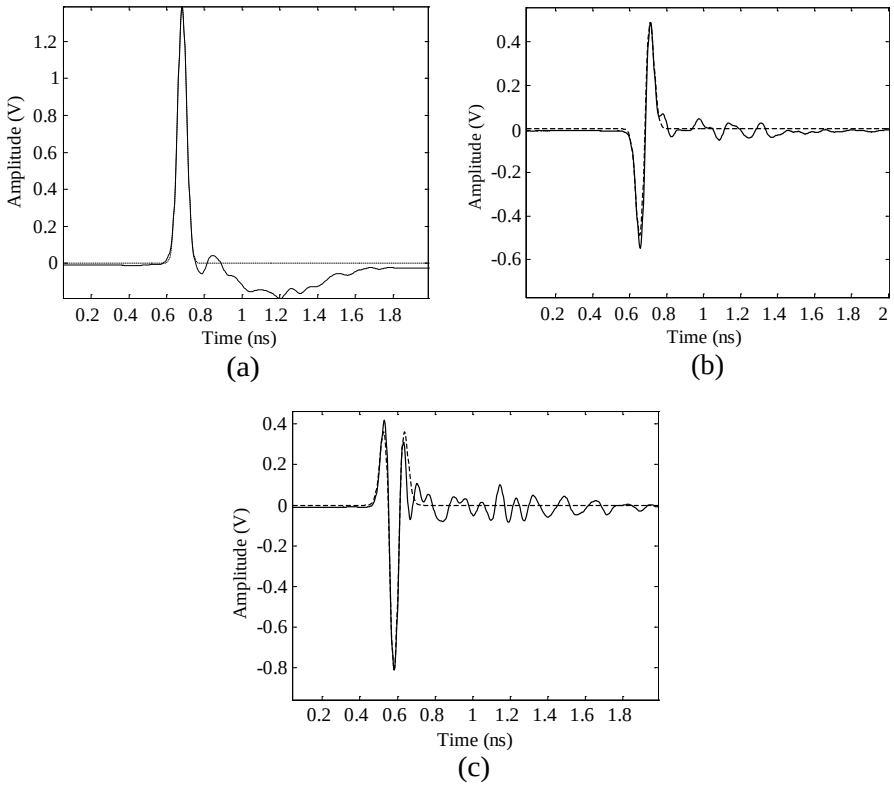

Figure 11. Theoretical (dashed line) and generated (solid line) (a) Gaussian pulse, (b) first derivative Gaussian pulse and (c) second derivative Gaussian pulse.

Gaussian pulses have been generated.

Figure 11(a) compares the generated (solid line) and theoretical (dashed line) Gaussian pulses with $\tau = 36$ psec. Figures 11(b) and 11(c) show generated (solid line) and theoretical (dashed line) first derivative Gaussian pulses with $\tau = 40$ psec and second derivative Gaussian pulses with $\tau = 45$ psec.

6. ENERGY PATTERN

As the antenna characteristics change with time and angle, it is not possible to define the field pattern of the antenna. The energy pattern can be defined for the transient response of the antenna as follows:

$$W_e = \int_{-\infty}^{\infty} |E(t)|^2 dt. \tag{20}$$

7. MEASUREMENTS

7.1. Monopole

Figure 12 shows a monopole antenna of length 10 cm with ground plane dimensions $15 \times 19\,\text{cm}^2$. All the measurements are carried out in an open room, which meet far field conditions.

The theoretical azimuth plane pattern is omnidirectional; however, the measurements show a variation of 0.6 dB in their energy at various angles. Figure 13(a) shows the measured and theoretical energy pattern of the monopole antenna for the Gaussian pulse excitation in the elevation plane.

Figure 12. Monopole antenna.

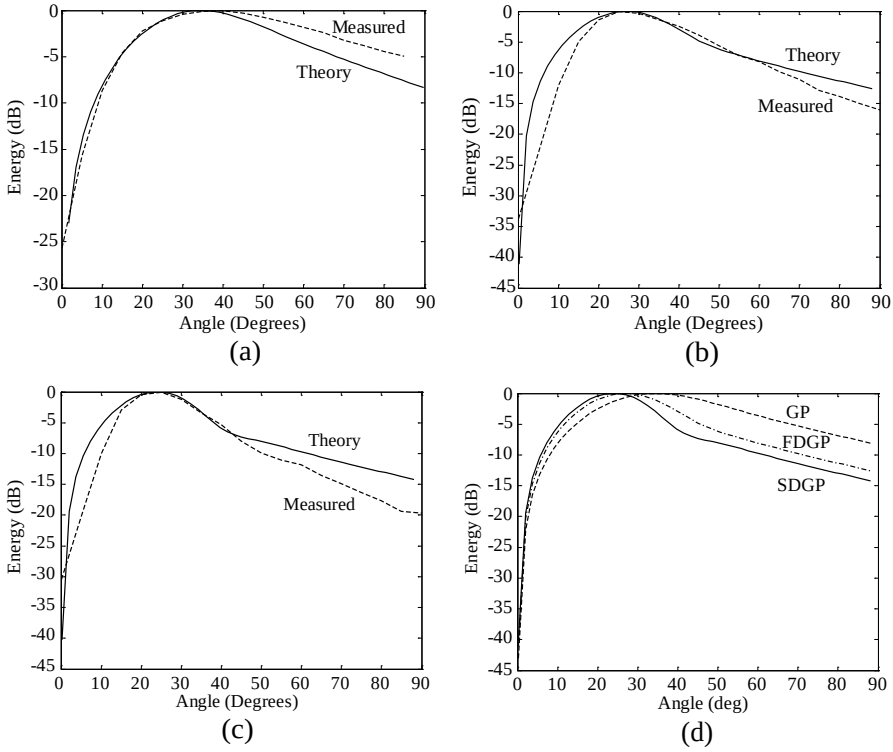

Figure 13. Energy pattern for (a) Gaussian pulse, (b) first derivative Gaussian pulse and (c) second derivative Gaussian pulse excitation in the elevation plane. Comparison of energy patterns for different pulse excitations is shown in (d).

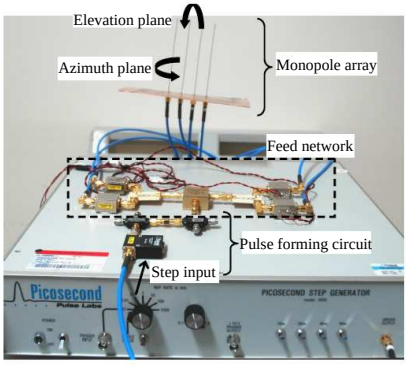

Figure 14. Monopole array antenna with feed circuit.

Figures 13(b) and 13(c) show the measured and theoretical energy patterns of the monopole in the elevation plane for first derivative and second derivative Gaussian pulse excitation. Figure 13(d) compares the energy pattern of the monopole for Gaussian pulse (GP), first derivative Gaussian pulse (FDGP) and second derivative Gaussian pulse (SDGP) excitation.

7.2. Array

Figure 14 shows the linear array of four monopoles with its feed circuit. The length of the each monopole is 10 cm and spacing between the monopoles is 2 cm. The feed network consists of pulse forming

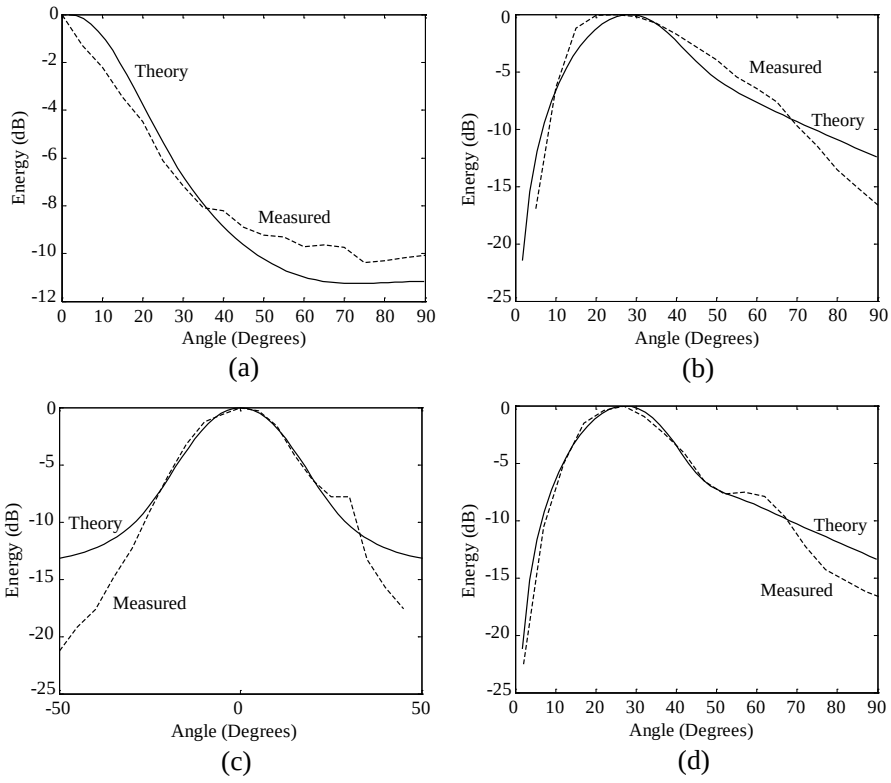

Figure 15. Energy pattern in the (a) azimuth and (b) elevation planes for first derivative Gaussian pulse excitation, and energy pattern in the (c) azimuth and (d) elevation planes for second derivative Gaussian pulse excitation.

circuit, whose output is divided into two halves, and each half is divided into two quarters. Each quarter is amplified and fed to the monopoles. Through this feed circuit all monopoles are excited with uniform amplitude and with no time delay amongst them. The power dividers and amplifiers are frequency dependent, and do not work at zero frequency. Therefore, Gaussian pulse excitation is not possible for the array configuration due to its strong DC component.

Figures 15(a) and 15(b) show the energy patterns of the four monopole linear arrays in the azimuth and elevation planes respectively for the first derivative Gaussian pulse excitation. Figures 15(c) and 15(d) show the energy patterns for second derivative Gaussian pulse excitation in the azimuth and elevation planes respectively.

8. CONCLUSION

The time domain analysis for the short pulse radiation due to a wire antenna is an efficient tool for UWB applications. This analysis is helpful in UWB array design and beam steering. The total radiation is the sum of the radiations from individual elements in the array. The shape of the radiated pulse can be controlled through the proper excitation of the array. Different Gaussian pulses have been generated with different pulse widths for exciting both monopole antennas and monopole arrays. The radiated pulses have been calculated for different Gaussian pulse excitations to the monopole and monopole arrays. Theoretical and measured radiated pulses and energy patterns are compared and found to show reasonable agreement.

REFERENCES

1. Taylor, J. D., *Introduction to Ultra-wideband (UWB) Radar Systems*, CRC Press, 1995.
2. Kanda, M., "Time-domain sensors and radiators," *Time-domain Measurements in Electromagnetics*, E. K. Miller (ed.), Ch. 5, Van Nostrand Reinhold, New York, 1986.
3. Griffith, H. D. and A. L. Cullen, "Sidelobe response of antennas to short pulse signals," *IEEE Radar Conference*, 85–90, 2003.
4. Balanis, C., *Antenna Theory Analysis and Design*, 2nd edition, John Wiley, 1982.
5. Samaddar, S. N. and E. L. Mokole, "Transient behavior of radiated and received fields associated with a resistively loaded dipole," *Ultra-wideband, Short-pulse Electromagnetics 4*, Kluwer Academic Publishers, 1999.

6. Wu, T. T. and R. W. P. King, "The cylindrical antenna with non-reflecting resistive loading," *IEEE Transactions on Antennas and Propagation*, Vol. 13, 369–373, 1965.
7. Cerny, P. and M. Mazanek, "Simulated transient radiation characteristics of optimized ultra wideband printed dipole antennas," *17th Int. Conf. Radioelektronika*, Brno, Czech Republic, Apr. 24–25, 2007.
8. Hartmann, R. B. and J. R. Bray, "Investigation of planar resonant dipole antennas for continuous-wave and ultra-wideband radar modes," *13th ANTEM / URSI Conf.*, Banff, Alberta, Feb. 15–18, 2009.
9. Krauss, J. D., *Electromagnetics*, 4th edition, McGraw Hill, 1992.
10. Smith, G. S., "Teaching antenna radiation from a time-domain perspective," *Am. J. Phys.*, Vol. 69, 829–844, 2001.
11. Tan, A. E.-C. and M. Y.-W. Chia, "Sub-nanosecond pulse forming network on SiGe BiCMOS for UWB communications," *IEEE Trans. MTT*, Vol. 54, 1019–1024, 2006.